Inorganic Chemistry

Article

pubs.acs.org/IC

Reversible Switching of Electronic Ground State in a Pentacoordinated Cu(II) 1D Cationic Polymer and Structural Diversity

Ashok Sasmal,[†] Eugenio Garribba,[‡] Corrado Rizzoli,[§] and Samiran Mitra*,[†]

[†]Department of Chemistry, Jadavpur University, Raja S.C. Mullick Road, Kolkata-700032, West Bengal, India

[‡]Department of Chemistry and Pharmacy, and Center for Biotechnology Development and Biodiversity Research, University of Sassari, Via Vienna 2, I-07100 Sassari, Italy

[§]Dipartimento di Chimica, Universitá degli Studi di Parma, Parco Area delle Scienze 17/A I-43124 Parma, Italy

Supporting Information

ABSTRACT: Two copper(II) polymeric complexes $\{[Cu(HPymat)(MeOH)](NO_3)\}_n$ (**1**) and $\{[Cu_4(Pymab)_4(H_2O)_4](NO_3)_4\}$ (**2**) were synthesized with the carboxylate-containing Schiff-base ligands $HPymat^-$ and $Pymab^-$ [H_2Pymat = (*E*)-2-(1-(pyridin-2-yl)-methyleneamino)terephthalic acid, HPymab = (*E*)-2-((pyridine-2-yl)methyleneamino)benzoic acid]. Complex **1** is a one-dimensional Cu(II) cationic polymeric complex containing free protonated carboxylic groups and nitrate anions as counterions. Complex **2** is a zero-dimensional tetranuclear cationic Cu(II) complex containing nitrate anions as counterions. Complex **1** shows rhombic electron paramagnetic resonance (EPR) spectra in the solid state at room temperature (RT) and 77 K and tetragonal EPR spectra in dimethyl sulfoxide (DMSO) and dimethylformamide (DMF) and "inverse" EPR spectrum in CH_3CN. Complex **2** shows rhombic EPR spectra in the solid state at RT and 77 K. But complex **2** shows tetragonal spectra in DMSO, DMF, and CH_3CN. Thermogravimetric analysis was also performed for both complexes **1** and **2**. Mean-square displacement amplitude analysis was carried out to detect librational disorder along the metal−ligand bonds in crystal structures.

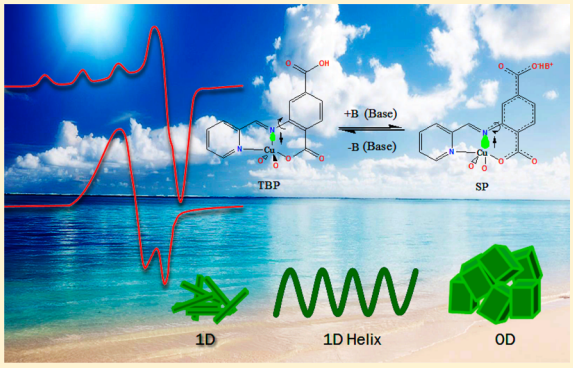

INTRODUCTION

Discovering temperature- and pressure-induced suitable molecules with a reversible switchable electronic ground state has been a major challenge to chemists as it strongly affects the reversible electron distribution within a material or molecule, as well as the arrangement of their atoms. This effect leads to some unusual phenomena in functional materials with switchable magnetic moments, low-temperature magnetic ordering, or in conducting and superconducting ceramics.[1−6] Two important factors, namely, geometry and ligand field strength, determine the electronic ground state in copper(II) complex. To switch the electronic ground state in a copper(II) complex, geometry and ligand field strength should be tuned by external stimuli. In octahedral Cu(II) complexes, switching of electronic ground states between $d_{x^2-y^2}$ and d_{z^2} can be performed by tetragonal compression or elongation. In the case of pentacoordinated Cu(II) complexes, geometry can exist in three different forms such as square pyramid (SQP), trigonal bipyramid (TBP), and intermediate between SQP and TBP. The SQP geometry can easily be transformed into TBP geometry by simple bonds rotation, as the $d_{x^2-y^2}$ electronic ground state is expected in SQP, whereas the d_{z^2} electronic ground state is expected in TBP (Scheme 1). In real systems, ideal geometries are rarely achieved. The electronic effect (electron donating or withdrawing) of substituents could be an important factor that may tune ligand field strength and selectively favor $d_{x^2-y^2}$ or d_{z^2} ground state in Cu(II) center.

In most of the octahedral Cu(II) complexes, the $d_{x^2-y^2}$ electronic ground state is found. The d_{z^2} electronic ground state is expected in a tetragonal compressed structure. To get the desired electronic ground state, distortion or transformation of geometry is needed. Three different types of structural distortion or transformation such as tetragonal, rhombic, and trigonal are possible in an octahedral system (Scheme 2). The trigonal prism or trigonal antiprism geometry (D_{3h} or D_{3d}) can be obtained, in principle, by trigonal distortion of octahedron along one of three C_3 axes. The required D_{3h} or D_{3d} geometries cannot be achieved due huge steric crowding. However, to the best of our knowledge, no copper complexes with trigonal prism or trigonal antiprism geometry are reported until now. In rhombic distortion, the electronic ground state can be described as a linear combination of $d_{x^2-y^2}$ and d_{z^2} where the ground state cannot be distinguishable.

Several octahedral Cu(II) complexes have been reported having inverted or quenched (pseudo) Jahn−Teller distortions by steric compression with d_{z^2} electronic ground state,[7−13] but electron paramagnetic resonance (EPR) spectra of the

Received: February 16, 2014
Published: June 9, 2014

   dx.doi.org/10.1021/ic500377w | *Inorg. Chem.* 2014, 53, 6665−6674

Scheme 1. Crystal Field Splitting for the (left) Octahedral and (right) Pentacoordinated Geometries of Copper(II) Complexes[a]

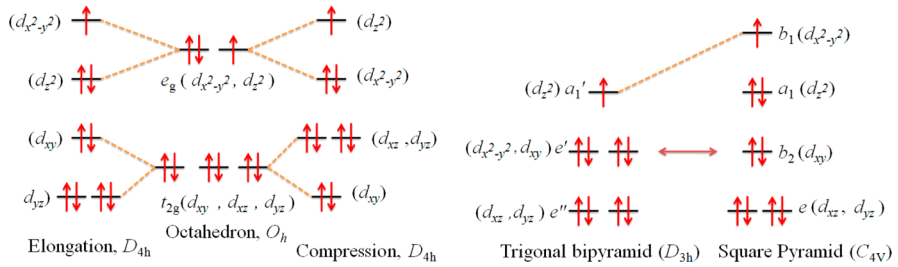

[a]The splitting between energy levels are qualitative only and are not drawn to scale.

Scheme 2. Various Types of Distortion in Octahedral and Pentacoordinated Complexes

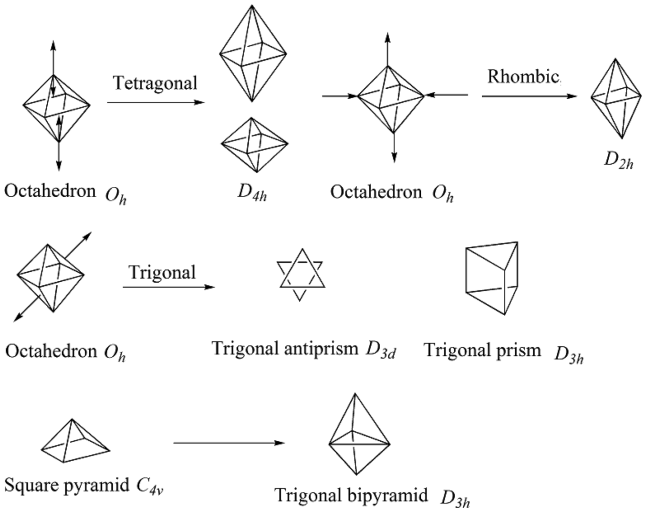

complexes represent rather rhombic distortion, which can be expressed by linear combination of d_{z^2} and $d_{x^2-y^2}$. Most of the complexes have been synthesized using various tridentate ligands, which are coordinated to metal center in meridional fashion, and substituents are projected outward. The ligand field strength rather than steric effect is responsible for the inverted or quenched (pseudo) Jahn–Teller distortions. The ligand field strength depends on basicity of donor atoms, which can be controlled by tuning resonance effect of phenyl ring by "out-of-plane" or "in-plane" rotation around the C–C bonds (Scheme 3). As structural distortion is very weak in an octahedral system, ligand field could play an important role in the electronic ground state.

We previously reported switching of electronic ground state in a pentacoordinated Cu(II) complex in solution.[14] Here we have chosen pentacoordinated Cu(II) systems to study switching of electronic ground state due to less steric crowding. In this study, we present the synthesis and structural characterization of two novel copper(II) one-dimensional (1D) cationic complex polymers, $\{[Cu(HPymat)(MeOH)](NO_3)\}_n$ (**1**) and $\{[Cu_4(Pymab)_4(H_2O)_4](NO_3)_4\}$ (**2**) using Schiff-base ligands $HPymat^-$ (L^2) and $Pymab^-$ (L^3) (Scheme 4). The electronic effect of substituents in electronic ground state and structural diversity will be discussed. EPR studies of the Cu(II) complexes will be presented to explore the nature of electronic ground state. TGA will be performed to analyze the stability for both complexes **1** and **2**. Mean-square displacement amplitude (MSDA) analysis will be carried out to detect librational disorder along the metal–ligand bonds in crystal structures.

EXPERIMENTAL SECTION

Materials. $Cu(NO_3)_2{\cdot}3H_2O$ was purchased from E. Merck, India. Anthranilic acid, 2-aminoterepthalic acid, and pyridine-2-carbaldehyde were purchased from Sigma-Aldrich. All solvents and reagents were of reagent grade and were used as received without further purification.

Synthesis of the Ligand H_2Pymat. 2-Aminoterephthalic acid (0.906 g, 5 mmol) and pyridine-2-carbaldehyde (0.535 g, 5 mmol)

Scheme 3. Various Meridional Tridentate Ligands

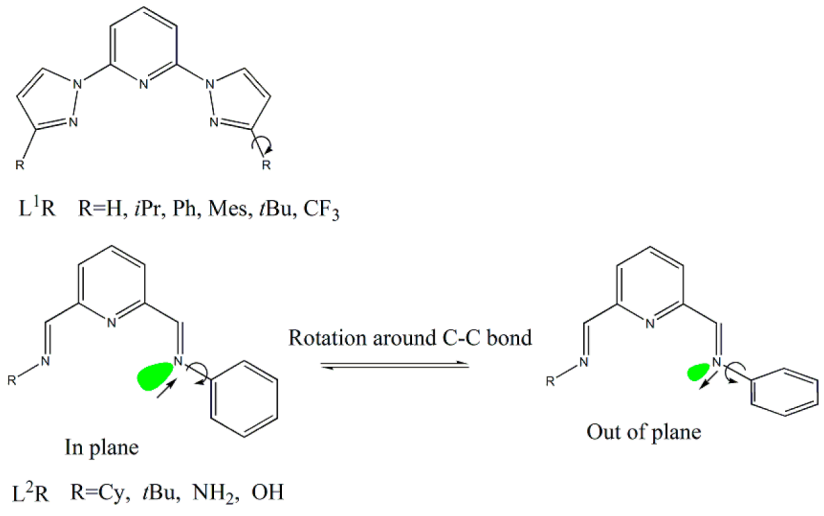

dx.doi.org/10.1021/ic500377w | Inorg. Chem. 2014, 53, 6665–6674

Scheme 4. Tridentate Ligand H_2Pyeat (L^1) (left),[14] H_2Pymat (L^2) (middle), and HPymab (L^3) (right)

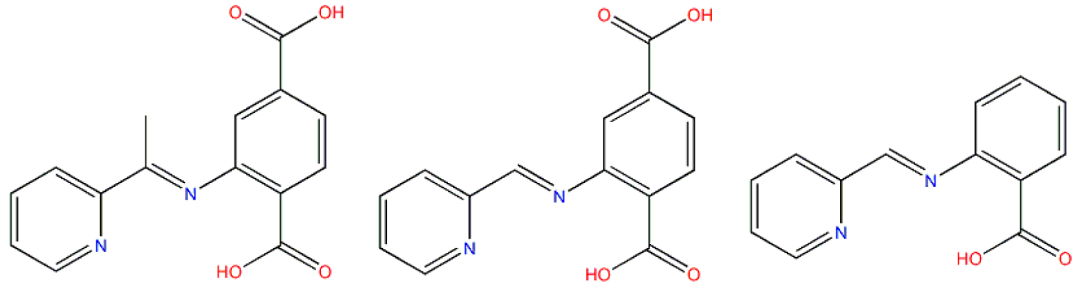

were taken in 25 mL of methanol. The reaction mixture was refluxed for 2 h. After 2 h the yellow reaction mixture was cooled to room temperature (RT) and filtered. Then filtrate was evaporated to dryness under vacuum. The yellow solid was purified by silica gel column chromatography using methanol and dichloromethane mixture in 1:4 ratio. Yield: 0.937 g (65%). Anal. Calcd (%) for $C_{14}H_{10}N_2O_4$ (M = 270 g mol^{-1}): C, 62.22; H, 3.73; N, 10.37. Found: C, 62.15; H, 3.60; N, 10.25. Fourier transform infrared (FT-IR) (KBr, cm^{-1}): 3393(b), 3072(s), 2530(b), 1910(b), 1701(s), 1626(s), 1589(s), 1467(s), 1437(w), 1408(w), 1295(m), 1277(m), 1231(s), 1126(s), 1094(m), 1054(m), 1010(s), 974(m), 916(s), 770(s), 756(s), 735(s), 679(s), 634(s), 559(w), 510(w), 485(m), 464(m). Ultraviolet−visible (UV−vis), CH_3OH (λ in nm (ε in dm^3 mol^{-1} cm^{-1})): 227 (9148), 254 (3333), 358 (1003). ^{1}H NMR (deuterated dimethyl sulfoxide (DMSO-d_6), 300 MHz) δ_H: 7.77 (d, J = 8.27, 1H), 7.38(s, 1H), 7.02(d, J = 8.27, 1H) ppm. Electrospray ionization mass spectrometry (ESI-MS), m/z: 271 [M + H$^+$, 30], 293 [M − H$^+$ + Na$^+$, 100].

Synthesis of the Ligand HPymab. Anthanilic acid (0.685 g, 5 mmol) and pyridine-2-carbaldehyde (0.535 g, 5 mmol) were taken in 25 mL of methanol. The reaction mixture was refluxed for 2 h. After 2 h the brown-colored reaction mixture was cooled to RT and filtered. Then filtrate was evaporated to dryness under vacuum. The oily brown mass was purified by silica gel column chromatography using methanol and dichloromethane mixture in 1:5 ratio. Yield: 0.854 g (70%). Anal. Calcd (%) for $C_{13}H_{10}N_2O_2$ (M = 226 g mol^{-1}): C, 69.02; H, 4.46; N, 12.38. Found: C, 68.95; H, 4.40; N, 12.25. FT-IR bands (KBr, cm^{-1}): 3319(s), 3067(m), 1926(w), 1717(s), 1684(s), 1611(s), 1499(s), 1437(s),1364(s), 1319(s), 1292(s), 1236(s), 1161(s), 1123(s), 1048(m), 832(s), 752(s), 695(s), 652(s), 633(s), 530(s). UV−vis, CH_3OH (λ in nm (ε in dm^3 mol^{-1} cm^{-1})): 332 (5619). ^{1}H NMR (DMSO-d_6, 300 MHz) δ_H: 9.98 (s, 1H, −COOH), 8.81 (d, J = 4.67, 1H, py-H), 8.04 (t, J = 7.62, 1H), 7.92(d, J = 6.74, 1H), 7.2(t, J = 7.68, IH), 6.7(d, J = 8.32, IH), 6.47(t, J = 7.47, IH), 6.28(s, 1H), 4.1(s, 1H) ppm. ESI-MS, m/z (M+, %): 227 [M + H$^+$, 70], 249 [M + Na$^+$, 40].

Synthesis of Complexes 1 and 2. *{[Cu(HPymat)(MeOH)](NO$_3$)}$_n$ (**1**).* $Cu(NO_3)_2{\cdot}3H_2O$ (0.241 g, 1 mmol) and ligand H_2Pymat (0.27 g, 1 mmol) were taken in 20 mL of methanol. The reaction mixture was refluxed for 1 h and filtered. The filtrate was left for slow evaporation. Green block-shaped single crystals were obtained after one week, suitable for single-crystal X-ray diffraction analysis. Yield: 0.36 g (70%). Anal. Calcd (%) for $C_{15}H_{13}CuN_3O_8$ (M = 426 g mol^{-1}): C, 42.21; H, 3.07; N, 9.84. Found: C, 42.10; H, 3.02; N, 9.80. FT-IR (KBr, cm^{-1}): 3482(b), 3056(w), 1698(s), 1578(s), 1539(s), 1475(w), 1411(s), 1287(s), 1254(s), 1131(s), 1107(s), 1029(s), 1014(s), 969(s), 947(s), 914(s), 856(s), 818(s), 776(s), 743(s), 702(s), 654(s), 502(m), 411(s). UV−vis, CH_3OH (λ in nm (ε in dm^3 mol^{-1} cm^{-1})): 240 (985), 339 (586), 355(676, sh). ESI-MS, m/z (M$^+$): 1107, [Cu_3(HPymat)$_3$ + CH_3CN + 3Na$^+$]; 1328, [Cu_4(HPymat)$_4$ + H$^+$]; 1660.03, [Cu_5(HPymat)$_5$ + H$^+$].

*{[Cu(Pymab)(H$_2$O)](NO$_3$)}$_4$ (**2**).* $Cu(NO_3)_2{\cdot}3H_2O$ (0.241 g, 1 mmol) and ligand HPymab (0.26 g, 1 mmol) were taken in 20 mL of methanol. The reaction mixture was refluxed for 1 h and filtered. The filtrate was left for slow evaporation. Green block-shaped single crystals were obtained after one week, suitable for single-crystal X-ray diffraction analysis. Yield: 0.4 g (70%). Anal. Calcd (%) for $C_{52}H_{52}Cu_4N_{12}O_{28}$ (M = 1547 g mol^{-1}): C, 40.37; H, 3.39; N, 10.86. Found: C, 40.26; H, 3.30; N, 10.80. FT-IR (KBr, cm^{-1}): 3368(m), 3097(s), 1590(s), 1555(s), 1476(s), 14447(m), 1411(m), 1384(m), 1235(s), 1203(m), 1159(m), 1102(s), 1052(m), 1022(s), 966(m), 923(s), 880(s), 841(s), 827(s), 775(s), 740(s), 716(s), 695(s), 647(m), 551(m), 525(m), 492(m), 457(m). UV−vis, CH_3OH (λ in nm (ε in dm^3 mol^{-1} cm^{-1})): 248 (5494), 335 (4699). ESI-MS, m/z (M$^+$): 1340.06, [Cu_4(Pymab)$_4{\cdot}4H_2O$ + 5Na$^+$ + H$^+$]

Physical Measurements. The FT-IR spectra (4000−400 cm^{-1}) of the ligand H_2Pymat and of complexes were recorded on a PerkinElmer RX-I FT-IR spectrophotometer in solid KBr matrix. The electronic spectra of the ligand and of the complexes were recorded at RT on a PerkinElmer λ 40 UV/vis spectrometer in methanol medium. Elemental analyses (C, H, and N) were carried out with a PerkinElmer 2400 II elemental analyzer. The ^{1}H NMR spectrum of the ligand was recorded on a Bruker 300 MHz FT-NMR spectrometer using trimethylsilane as internal standard in DMSO-d_6. ESI-MS experiments were performed with a Waters QtoF Model YA 263 spectrometer in positive ion ESI mode. Mass spectra for complex **1** were taken in acetonitrile and dimethylformamide (DMF) mixture, but mass spectra for complex **2** were taken in acetonitrile medium. EPR spectra were recorded from 0 to 10 000 G in the temperature range of 77−298 K with an X-band (9.4 GHz) Bruker EMX spectrometer. EPR parameters reported in the text were obtained by simulating the spectra with the computer program Bruker WinEPR SimFonia.[15] Thermogravimetric analyses (TGAs) were carried out with a heating rate of 10 °C min^{-1} with a Mettler-Toledo Star TGA/SDTA-851 thermal analyzer system in a dynamic atmosphere of N_2 (flow rate 80 mL min^{-1}), using alumina crucibles in a temperature range of 25−450 °C.

X-ray Crystallography. A good-quality single crystal of **1** and **2** were mounted on a Bruker Smart 1000 CCD and Bruker APEX-II CCD diffractometer equipped with graphite monochromatized Mo Kα radiation (λ = 0.710 73 Å) fine-focus sealed tube. For **1** and **2**, intensity data were collected using ω scan at 294 K. Unit cell refinement and data reduction were performed using the Bruker SAINT software.[16] Multiscan absorption corrections were applied empirically to the intensity values (Tmin = 0.788 and Tmax = 0.885 for **1**, Tmin = 0.814 and Tmax = 0.940 for **2**) using SADABS.[16] The structures were solved by direct methods using the program SIR97[17] and were refined with full-matrix least-squares based on F^2 using program SHELX 97-L.[18] The crystal of **1** used for X-ray analysis exhibited a merohedric twinning by rotation of 180° around the b* axis (twinning matrix −1 0 0/0 1 0/0 0−1). The Flack parameter of 0.875(11) was refined in the full matrix least-squares process using the TWIN/BASF option. In **2**, two out of four crystallographically independent nitrate anions have full occupancy and were refined anisotropically (Figure S2, Supporting Information). A third nitrate anion was found to be disordered about two different sites having 2-fold symmetry (Figure S3, Supporting Information). In each site the anion assumes four orientations sharing the oxygen atoms. The fourth nitrate anion is disordered over two orientations about two independent sites having inversion symmetry, the sites being shared with a disordered water molecule (Figure S4, Supporting Information). The refinement of the disordered nitrate anions was carried out by applying an occupancy of 0.5 to atoms N13, N14, O20, O21, O23, O24, O26, O28, O29, and O30, an occupancy of 0.25 to atoms N11A,

dx.doi.org/10.1021/ic500377w | Inorg. Chem. 2014, 53, 6665−6674

Table 1. Crystallographic Data and Structure Refinement for 1 and 2

empirical formula	$C_{15}H_{13}CuN_3O_8$	C_{52} $H_{52}Cu_4N_{12}O_{28}$
formula weight	426.82	2986.34
crystal system	orthorhombic	monoclinic
space group	$Pna2_1$ (No. 33)	$C2/c$ (No. 15)
temperature	294	295
a (Å)	14.728(2)	21.452(2)
b (Å)	14.876(2)	21.421(2)
c (Å)	7.4484(11)	27.277(3)
β (deg)	90	107.912(2)
V (Å^3)	1631.9(4)	11927(2)
Z	4	4
d_{calc} (g cm^{-3})	1.737	1.663
μ (mm^{-1})	1.392	1.502
F(000)	868	6064
crystal size (mm^3)	0.10 × 0.14 × 0.22	0.05 × 0.11 × 0.14
θ range (deg)	1.4−25.5	1.4−25.3
measured reflections	18 238	24 915
independent reflections	3014	10 811
R(int)	0.033	0.047
observed data [$I > 2\sigma(I)$]	2883	6826
goodness-of-fit on F^2	1.05	1.04
final R indices [$I > 2\sigma(I)$]	$R1$ = 0.0243,wR^2 = 0.0631	$R1$ = 0.0524; wR^2 = 0.1519
R indices (all data)	$R1$ = 0.0258, wR^2 = 0.0620	$R1$ = 0.0948; wR^2 = 0.1300
ρ_{min} and ρ_{max} (e Å^{-3})	−0.18 and 0.41	−0.51 and 1.43
Flack parameter	0.875(11)	

N11B, N12A, N12B, O19A, O19B, O22A, and O22B, and by constraining the N−O and O···O distances to be 1.23(1) and 2.13(2) Å, respectively. All disordered O and N atoms were refined anisotropically except for atoms N11A, N11B, N12A, and N12B for which the anisotropic refinement was unsuccessful. During the refinement, FLAT, SIMU, ISOR, and EADP restraints were applied. The hydroxy H atoms in **1** were located in a difference Fourier map and refined freely. The water H atoms in **2** were placed in calculated positions to maximize geometrically feasible hydrogen bonding interactions and were refined as riding, with O−H = 0.82 Å and with U_{iso}(H) = 1.5U_{eq}(O). C-bound hydrogen atoms in **1** and **2** were placed geometrically and refined using a riding model approximation, with C−H = 0.93−0.96 Å, and with U_{iso}(H) = 1.2U_{eq}(C) or 1.5U_{eq}(C) for methyl H atoms. A rotating-group model was used for the methyl group in **1**. The anisotropic displacement ellipsoid plots and crystallographic illustrations for **1** and **2** were prepared using the programs ORTEP[19a] and SCHAKAL.[19b] Crystallographic data and structure refinement parameters for **1** and **2** are summarized in Table 1.

RESULTS AND DISCUSSION

Description of Crystal Structures. *{[Cu(HPymat)(MeOH)](NO$_3$)}$_n$ (**1**).* An ORTEP view of the asymmetric unit of **1** with atom labels is shown in Figure 1. The complex **1** crystallizes in the $Pna2_1$ space group of the orthorhombic crystal system. Selected bond lengths and angles are listed in Table 2. The asymmetric units of **1** contain one L^2 (HPymat$^-$) ligand, one Cu(II) atom, one NO_3^- anion, and one CH_3OH molecule. The crystal structure of **1** is 1D cationic polymer having lattice nitrate anions to balance the charge of the complex (Figure 1). The geometry around the Cu(II) ions can be defined as a nearly perfect SQP with an Addison parameter τ of 0.03.[20] The coordination positions in the basal plane are occupied by the N1, N2, O3, and O4^i of HPymat$^-$ ligand, whereas the axial position is occupied by a methanol molecule [Cu1−O8, 2.354(2) Å]. The Cu−O and Cu−N equatorial bond lengths are in the range of 1.9182(16)−1.9448(15)Å and

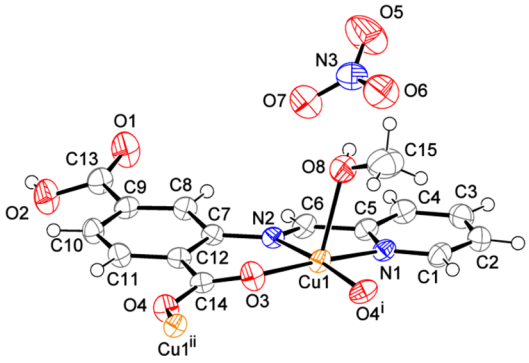

Figure 1. Asymmetric unit of complex **1**, with displacement ellipsoids drawn at the 50% probability level. Symmetry codes: (i) 1 − x, −y, 1/2 + z; (ii) 1 − x, −y, −1/2 + z.

Table 2. Bond Distances (Å) and Angles (deg) in 1

atoms[a]	distance	atoms[a]	angle
Cu1−O3	1.9182(16)	O3−Cu1−O8	100.22(7)
Cu1−O8	2.354(2)	O3−Cu1−N1	172.49(7)
Cu1−N1	1.986(2)	O3−Cu1−N2	91.58(6)
Cu1−N2	2.0016(17)	O3−Cu1−O4^i	86.96(6)
Cu1−O4^i	1.9448(15)	O8−Cu1−N1	85.65(8)
		O8−Cu1−N2	98.25(7)
		O4^i−Cu1−O8	87.52(7)
		N1−Cu1−N2	82.88(7)
		O4^i−Cu1−N1	98.05(7)
		O4^i−Cu1−N2	174.22(7)

[a]Symmetry code: (i) 1 − x, −y, 1/2 + z.

1.986(2)−2.0016(17) Å, respectively. The copper(II) ions are bridged consecutively by through *syn-anti* fashion of carboxylate groups extending along the c axis (Figure 2). Complex **1** contains also a free protonated carboxylic acid group projected

dx.doi.org/10.1021/ic500377w | Inorg. Chem. 2014, 53, 6665−6674

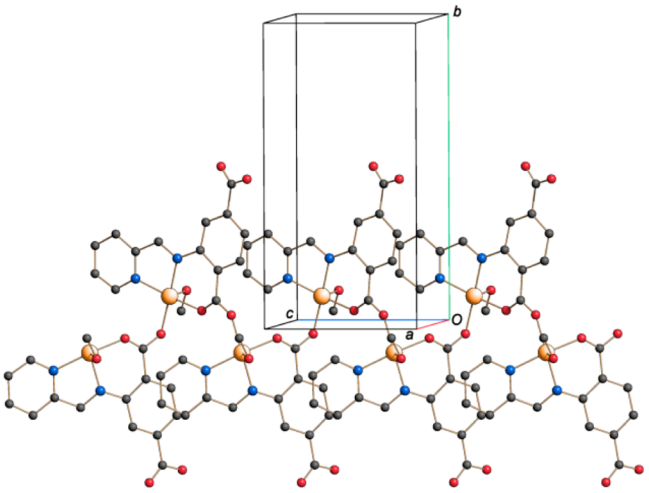

Figure 2. Partial crystal packing of complex **1** showing the cationic polymeric chain extending along the *c* axis. Nitrate anions and hydrogen atoms are omitted.

outside from the chains. In the crystal packing, the nitrate anions are connected to the coordinated methanol molecule and carboxylic groups through O7—H2O···O2 and O6—H8O···O8 hydrogen interactions (Figure 3). In addition, further

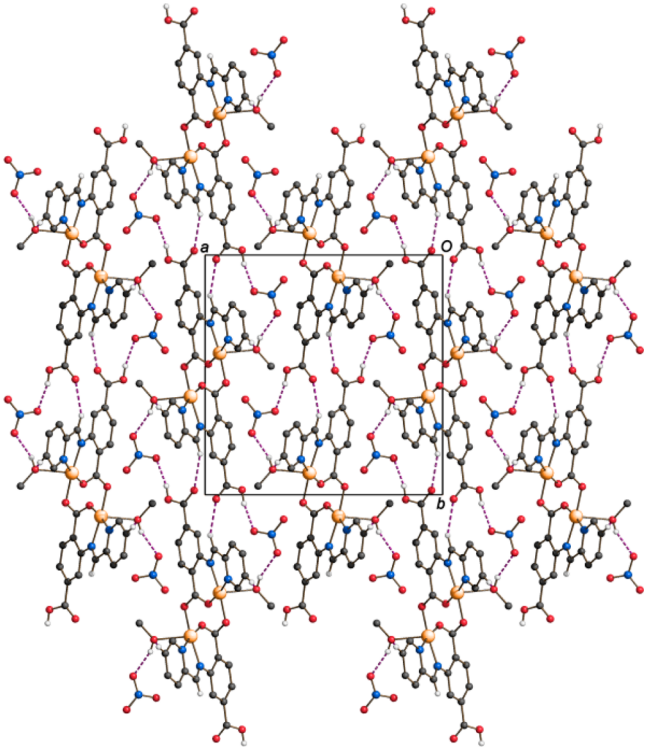

Figure 3. Crystal packing of complex **1** viewed down the *c* axis. Hydrogen bonds are shown as dashed lines.

nonclassical hydrogen interactions are observed between H atoms attached to the aromatic C6 carbon atom and O1 atom of carboxylic acid group (Table S1, Supporting Information).

Complex 2. *{[Cu_4(Pymab)$_4$(H_2O)$_4$](NO_3)$_4$} (**2**).* Complex **2** crystallizes in *C*2/*c* space group of the monoclinic crystal system. Selected bonding parameters are listed in Table 3. The asymmetric units of **2** contain four L^3 ($Pymab^-$) ligands, four Cu(II) atoms, four NO_3^- anions, and four H_2O molecules. An

Table 3. Bond Distances (Å) and Angles (deg) in 2

atoms	distance	atoms	angle
Cu1—O8	1.931(3)	Cu3—O4	1.929(3)
Cu1—O1	1.956(4)	Cu3—O5	1.946(4)
Cu1—N2	1.969(4)	Cu3—N6	1.975(4)
Cu1—N1	2.015(4)	Cu3—N5	2.015(4)
Cu1—O9	2.188(4)	Cu3—O11	2.166(4)
Cu2—O2	1.933(3)	Cu4—O6	1.932(3)
Cu2—O3	1.952(3)	Cu4—O7	1.945(3)
Cu2—N4	1.974(4)	Cu4—N8	1.969(4)
Cu2—N3	2.016(4)	Cu4—N7	2.006(4)
Cu2—O10	2.181(4)	Cu4—O12	2.172(4)
O8—Cu1—O1	90.64(15)	O4—Cu3—O5	90.62(15)
O8—Cu1—N2	176.53(16)	O4—Cu3—N6	176.23(16)
O1—Cu1—N2	88.79(16)	O5—Cu3—N6	89.05(16)
O8—Cu1—N1	100.65(16)	O4—Cu3—N5	100.49(17)
O1—Cu1—N1	144.71(16)	O5—Cu3—N5	145.35(17)
N2—Cu1—N1	81.73(17)	N6—Cu3—N5	81.84(18)
O8—Cu1—O9	88.58(15)	O4—Cu3—O11	87.44(15)
O1—Cu1—O9	101.71(16)	O5—Cu3—O11	102.72(16)
N2—Cu1—O9	88.19(16)	N6—Cu3—O11	88.97(16)
N1—Cu1—O9	111.80(17)	N5—Cu3—O11	110.41(17)
O2—Cu2—O3	90.25(15)	O6—Cu4—O7	90.82(15)
O2—Cu2—N4	176.72(16)	O6—Cu4—N8	175.78(16)
O3—Cu2—N4	89.21(15)	O7—Cu4—N8	89.06(16)
O2—Cu2—N3	100.48(17)	O6—Cu4—N7	100.77(17)
O3—Cu2—N3	144.63(17)	O7—Cu4—N7	145.25(17)
N4—Cu2—N3	81.78(18)	N8—Cu4—N7	81.64(17)
O2—Cu2—O10	88.66(15)	O6—Cu4—O12	87.02(15)
O3—Cu2—O10	102.20(16)	O7—Cu4—O12	102.29(17)
N4—Cu2—O10	88.29(16)	N8—Cu4—O12	88.89(16)
N3—Cu2—O10	111.57(16)	N7—Cu4—O12	110.87(18)

ORTEP view of the asymmetric unit of **2** with atom labeling is shown in Figure 4. The crystal structure of complex **2** consists of discrete tetranuclear $[Cu_4(L^3)_4(H_2O)_4]^{4+}$ cations and four isolated NO_3^- anions in the ratio of 1:4. The tetranuclear cationic units are formed by four cationic $\{Cu(L^3)(H_2O)\}^+$ units bridged by *syn-anti* fashion of carboxylate groups. The basal plane of Cu(II) ions are occupied by N, N, O donors from the tridentate chelating ligand $Pymab^-$, O donor of a carboxylate group from an adjacent $\{Cu(L^3)(H_2O)\}^+$ unit. The axial positions are occupied by one water molecule. The coordination environment around Cu(II) ion is intermediate between SQP and TBP geometry with Addison parameters[20] τ = 0.530, 0.534, 0.514, and 0.508 for Cu1, Cu2, Cu3, and Cu4, respectively. The four Cu(II) atoms share the four corners of the virtual tetrahedron, where the Cu···Cu separation varies from 4.7041(9) to 4.7632(9) Å along the bridging edges and from 5.169(1) to 5.178(1) Å along the nonbridging edges of copper centers. All copper atoms in **2** have the same CuN_2O_3 coordination environment in which the basal Cu—N and Cu—O bond distances vary between 1.969(4)—2.016(4) Å and 1.929(3)—1.956(4) Å, respectively. The axial Cu—OH_2 bond distance variations are in the range of 2.166(4)—2.188(4) Å. In the crystal (Figure S5, Supporting Information), cations and anions are linked by classical O—H···O and nonclassical C—H···O hydrogen bonds into a three-dimensional network (Table S2, Supporting Information).

Comparison of Structures. The comparison of the structures of **1**, **2**, and **3** is shown in Table 4. Complexes **1**, **2**, and **3** have three different structural moieties, such as 1D

dx.doi.org/10.1021/ic500377w | *Inorg. Chem.* 2014, 53, 6665—6674

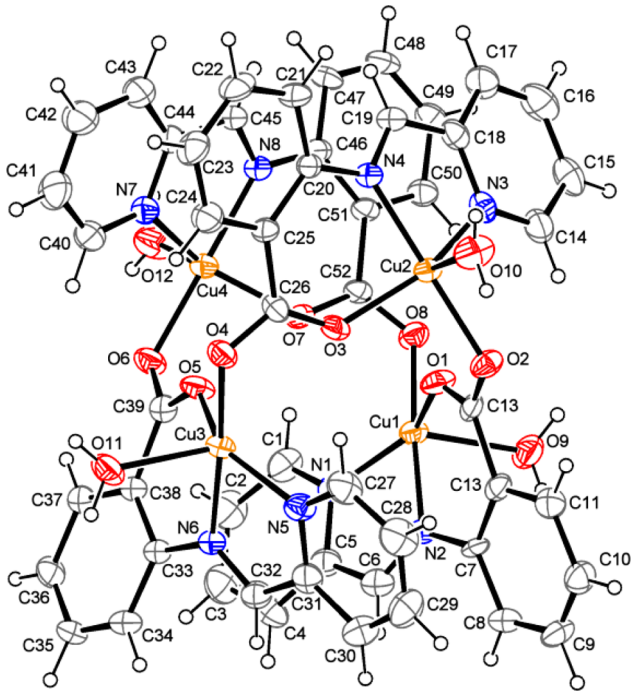

Figure 4. Structure of the cation in complex **2**, with displacement ellipsoids drawn at the 30% probability level.

discrete dinuclear complex, 1D helical polymer, and zero-dimensional (0D) discrete tetranuclear complex, respectively. Each complex contains a similar tridentate ligand system with different substituent such as −Me and −COOH. So, electronic effects of substituents may be a cause of structural diversity in Cu(II) complexes.

Mean-Square Displacement Amplitude Analysis. The EPR spectra of **1** and **2** in the solid state are similar in pattern at RT and 77 K (see below) indicating static nature of crystal structures, and/or the Cu center in the crystal lies in a special position, so that the Cu−ligand bond lengths will remain temperature-invariant. So, a thermal ellipsoid analysis is carried out to determine the presence or absence of librational disorder. A much more sensitive way of detecting librational disorder in a structure is through a mean-square displacement amplitude (MSDA) analysis. This analysis extracts from the thermal ellipsoids the amplitude of vibration of an atom along each of the bonds. The MSDA for a given atom, parallel to a given chemical bond, is given by eq 1:

$$\mathrm{MSDA} = \frac{\sum_{i=1}^{3}\sum_{j=1}^{3} U_{ij} n_i n_j}{|n|^2} \quad (1)$$

where U_{ij} is an element of the 3 × 3 matrix of thermal parameters and n_i and n_j are elements of the vector describing the bond. The difference between the MSDA values for the two atoms in a given chemical bond (ΔMSDA) will then be proportional to the degree of interatomic libration along that bond (eq 2)

$$\Delta\mathrm{MSDA} = \mathrm{MSDA(ligand)} - \mathrm{MSDA(metal)} \quad (2)$$

The parameter ΔMSDA is indicated with the abbreviation $\langle d^2 \rangle$, with units of Å^2. All ΔMSDA data in this article are quoted as $\langle d^2 \rangle$. MSDA analyses can be carried out from most standard crystallographic output files, when the atoms of interest have been refined anisotropically, using the program THMA11. The crystallographic Cu−N/O bond lengths and the corresponding $\langle d^2 \rangle$ values of **1** and **2** at 293 K are shown in Scheme 5.

Scheme 5. Crystallographic Cu−N/O Bond Lengths and Corresponding ⟨× 10^4 d^2⟩ Values in Square Brackets of 1 and 2 at 293 K

Complex 1 **T=294K**

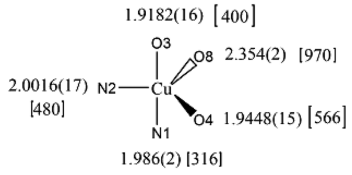

Complex 2

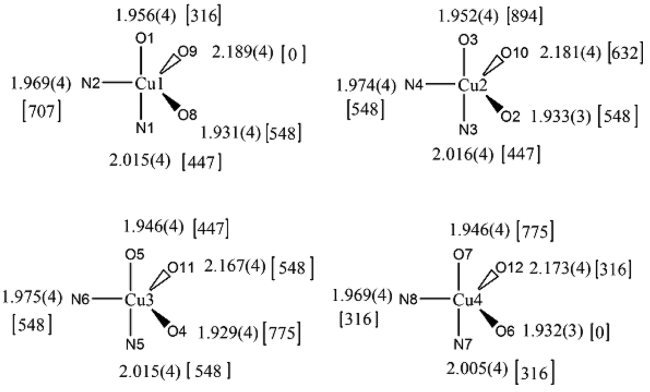

Table 4. Comparison of Structural Parameters

	[Cu$_2$(μ-Cl)$_2$(L^1)$_2$][14] (**3**)	complex **1**	complex **2**
substituents	−COOH, −Me	−COOH	
dimension	1D	1D helix	0D
Addison parameter (τ)	0.65	0.03	0.51−0.53
dihedral angles (deg)[a]	48.14(3)	12.7(3)	25.7(7)−29.4(7)
Cu−N$_{im}$ bond lengths (Å)	1.974(2)	2.0016(17)	1.969(4)−1.975(4)
Cu−N$_{Py}$ bond lengths (Å)	2.003(2)	1.986(2)	2.005(4)−2.016(4)
Cu−O$_{chelate}$ bond lengths (Å)	1.958 (2)	1.9182(16)	1.952(4)−1.956(4)
Cu−O$_{bridging}$ bond lengths (Å)		1.9448(15)	1.929(4)−1.933(3)
−C═N− bond lengths (Å)	1.286(3)	1.269(3)	1.280(7)
C−N bond lengths (Å)	1.420(3)	1.420(3)	1.420(6)−1.433(6)
C−N═C angles (deg)	124.5(2)	121.8(2)	122.2(5)

[a]Between the least-squares mean planes of the imine group and benzene ring.

dx.doi.org/10.1021/ic500377w | Inorg. Chem. 2014, 53, 6665−6674

There is a wide spread of $\langle d^2 \rangle$ values for the five Cu−N/Cu−O bonds, for each complex. The $\langle d^2 \rangle$ (970) for the Cu−O(MeOH) bonds is particularly high in **1** compared with $\langle d^2 \rangle$ (498_{av}) for the Cu−O(H_2O) bonds in **2**. So, methanol evaporates at lower temperature than water from complex **1** (see below). The $\langle d^2 \rangle$ for the Cu−N_{im} is much higher than that for the Cu−$O_{chelate}$ bond in **1**, indicating that the Cu−N_{im} bond is more sensitive to the nature of the electronic ground state and structural distortion of copper(II) complex. The average wide spread of the $\langle d^2 \rangle$ values for the five Cu−N/Cu−O bonds in **2** Cu−N_{im} = 530; Cu−$O_{chelate}$ = 608; Cu−N_{py} = 440; Cu−$O_{bridging}$ = 624 is higher than it is in complex **1**. This indicates that complex **1** is more thermally stable than complex **2**. Complex **2** is disintegrated at a lower temperature than complex **1**.

Electron Paramagnetic Resonance Study. The EPR spectra of the polycrystalline complex **1** were recorded at 298 and 77 K. The two spectra are shown in Figure 5. The spectra

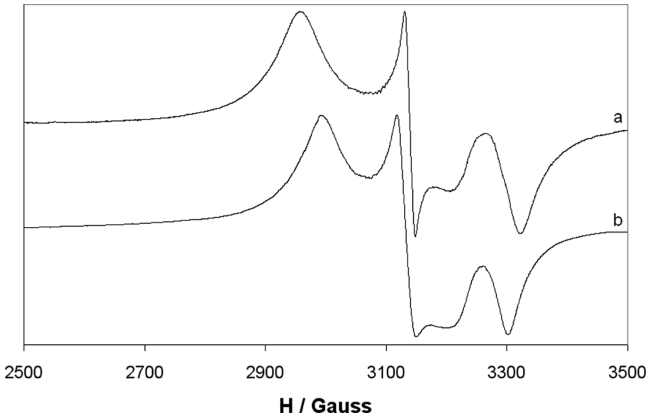

Figure 5. X-band EPR spectra of the polycrystalline complex **1** at (a) 298 and (b) 77 K.

are "rhombic" with three g values in the order of $g_x > g_y > g_z > g_e$ (Table 5). No resonances below 2800 and above 3400 G and no half-field transition were detected. These spectra were originated by a ground state Ψ, which can be described as a linear combination of $d_{x^2-y^2}$ and d_{z^2} orbitals, $\Psi = c_1|d_{z^2}\rangle + c_2|d_{x^2-y^2}\rangle$.[21,22] For these situations, the parameter R ($R = (g_z - g_y)/(g_x - g_y)$), with $g_x > g_y > g_z$, is indicative of the predominance of the d_{z^2} ($c_1 > c_2$) or $d_{x^2-y^2}$ orbital ($c_2 > c_1$).[23] If $R > 1$, the greater contribution to the ground state arises from the d_{z^2} orbital, and if $R < 1$, this arises from the $d_{x^2-y^2}$ orbital.[23] For a pentacoordinated Cu(II) structure, the d_{z^2} ground state is associated with a TBP structure, whereas $d_{x^2-y^2}$ is associated with an SQP geometry.[22]

Notice in Table 5 that the R value is close to the critical value of 1; it is slightly larger than 1 at 298 K and slightly smaller than 1 at 77 K. Compound **1** is expected to afford an $S = 1/2$ spectrum. This means that a strong mixing between the $d_{x^2-y^2}$ and d_{z^2} orbitals exists and that variations in temperature can cause slight structural changes in bond length and angles, which modify the contribution of $d_{x^2-y^2}$ and d_{z^2} in the singly occupied molecular orbital (SOMO) that bears the unpaired electron. Similar temperature-induced switching of the electronic ground state is now well-established in a limited number of Cu(II) compounds.[1]

When **1** is dissolved in an organic solvent two different results are obtained (Figure 6). When the solvent is DMF or

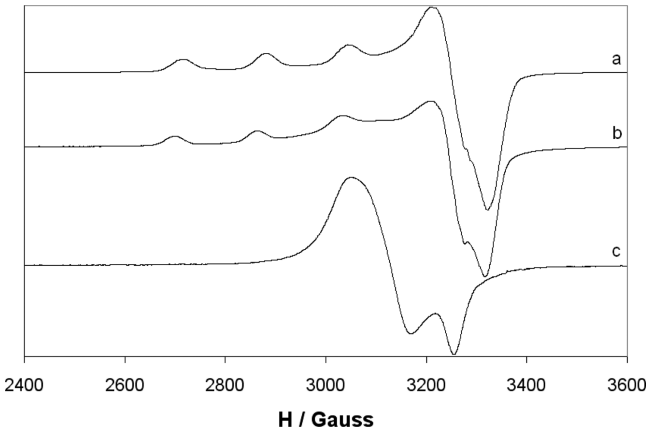

Figure 6. Anisotropic X-band EPR spectra of complex **1** dissolved in (a) DMF, (b) DMSO, and (c) CH_3CN.

DMSO (Figure 6a,b), a tetragonal spectrum is obtained with $g_z > g_x = g_y > g_e$ (Table 6). At these experimental conditions, the deprotonation of the noncoordinated carboxylic group takes place, and the ground state is $d_{x^2-y^2}$. On the contrary, when the solvent is CH_3CN (Figure 6c), an "inverse" spectrum is detected with $g_x = g_y > g_z > g_e$, and the ground state is d_{z^2}. In other words, the geometry appears to be distorted SQP in DMSO and DMF but distorted TBP in CH_3CN. The −COOH group is deprotonated in the $-COO^-$ form in DMSO (DMF), whereas it remains protonated in CH_3CN. This has been fully demonstrated for H_2Pyeat;[14] in particular, the addition of a base in CH_3CN causes the transformation of the distorted TBP geometry of the Cu(II) center into the distorted SQP geometry (Scheme 6).[14] The electron-withdrawing effect of the carboxylic acid group weakens the Cu−O and/or Cu−N bonds and induces the flip of electronic ground state in Cu(II) ion from $d_{x^2-y^2}$ to d_{z^2}, analogously to what was observed for the Cu(II) complex formed by H_2Pyeat = (*E*)-2-((1-(pyridin-2-yl)methyleneamino)terephthalic acid.[14]

Table 5. EPR Parameters of the Polycrystalline Solid Complexes 1 and 2 at 298 and 77 K

complex[a]	temperature	g_x	g_y	g_z	R	ground state	refs.
$[Cu_2(\mu\text{-Cl})_2(HPyeat)_2]$ (**3**)	298 K	2.249	2.093	2.035	0.37	$c_1\|d_{z^2}\rangle + c_2\|d_{x^2-y^2}\rangle$ ($c_1 < c_2$)	14
$[Cu_2(\mu\text{-Cl})_2(HPyeat)_2]$ (**3**)	77 K	2.257	2.094	2.039	0.34	$c_1\|d_{z^2}\rangle + c_2\|d_{x^2-y^2}\rangle$ ($c_1 < c_2$)	14
1	298 K	2.248	2.148	2.038	1.10	$c_1\|d_{z^2}\rangle + c_2\|d_{x^2-y^2}\rangle$ ($c_1 > c_2$)	this work
1	77 K	2.276	2.143	2.025	0.89	$c_1\|d_{z^2}\rangle + c_2\|d_{x^2-y^2}\rangle$ ($c_1 < c_2$)	this work
2	298 K	2.259	2.147	2.038	1.03	$c_1\|d_{z^2}\rangle + c_2\|d_{x^2-y^2}\rangle$ ($c_1 > c_2$)	this work
2	77 K	2.300	2.145	2.005	1.11	$c_1\|d_{z^2}\rangle + c_2\|d_{x^2-y^2}\rangle$ ($c_1 > c_2$)	this work

[a] H_2Pyeat is (*E*)-2-((1-(pyridin-2-yl)ethylidene)amino)terephthalic acid.

dx.doi.org/10.1021/ic500377w | Inorg. Chem. 2014, 53, 6665−6674

Table 6. EPR Parameters of the Polycrystalline Solid Complex 1 and 2 Dissolved in Organic Solvents

complex[a]	solvent	g_z	A_z[b]	g_y	A_y[b]	g_x	A_x[b]	ground state	refs.
$[Cu_2(\mu\text{-}Cl)_2(HPyeat)_2](3)$	DMF	2.275	151	2.068	18	2.052	14	$d_{x^2-y^2}$	14
$[Cu_2(\mu\text{-}Cl)_2(HPyeat)_2](3)$	DMSO	2.268	166	2.061	14	2.061	14	$d_{x^2-y^2}$	14
$[Cu_2(\mu\text{-}Cl)_2(HPyeat)_2](3)$	CH_3CN	2.062	54	2.251	35	2.251	35	d_{z^2}	14
1	DMF	2.269	173	2.061	14	2.061	14	$d_{x^2-y^2}$	this work
1	DMSO	2.276	174	2.064	14	2.064	14	$d_{x^2-y^2}$	this work
1	CH_3CN	2.064		2.212		2.212		d_{z^2}	this work
2	DMF	2.264	177	2.057	17	2.057	17	$d_{x^2-y^2}$	this work
2	DMSO	2.274	178	2.064	16	2.064	16	$d_{x^2-y^2}$	this work
2	CH_3CN	2.277	176	2.063	14	2.063	14	$d_{x^2-y^2}$	this work

[a] H_2Pyeat is (*E*)-2-((1-(pyridin-2-yl)ethylidene)amino)terephthalic acid. [b] A_x, A_y, and A_z values reported in 10^{-4} cm^{-1}.

Scheme 6. Simple Deprotonation of Carboxylic Acid Groups Causes the Transformation of the Distorted Trigonal Bipyramidal Geometry of Cu(II) Center into the Distorted Square Pyramidal Geometry

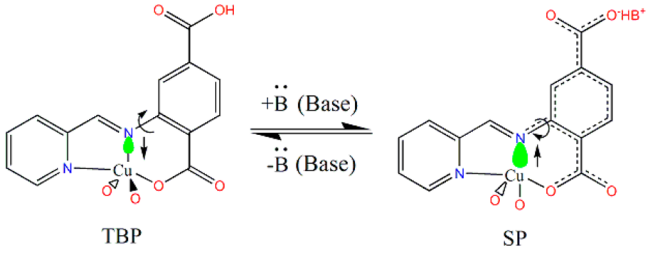

In Figure 7, the EPR spectra measured in mixtures of CH_3CN/DMSO are shown. In particular, with increasing the amount of DMSO, the inverse spectrum detected in CH_3CN transforms into the tetragonal one. This confirms the effect of solvent in determining the ground state through the protonation/deprotonation process of the carboxylic group (Scheme 6).

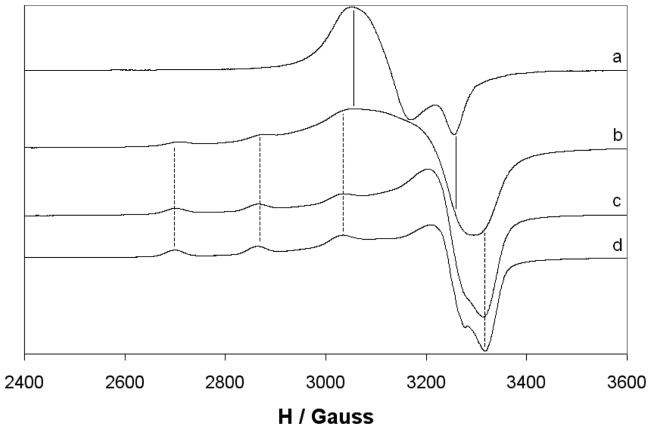

Figure 7. Anisotropic X-band EPR spectra of complex **1** dissolved in (a) CH_3CN; (b) mixture of CH_3CN/DMSO 3:1 v/v; (c) mixture of CH_3CN/DMSO 1:3 v/v, and (d) DMSO. The full and dotted lines indicate the resonances of the species with d_{z^2} and $d_{x^2-y^2}$ ground states, respectively.

Complex **2** is formed by the ligand obtained from condensation of anthranilic acid and pyridine-2-carbaldehyde. It does not have the carboxylic group in *para* position to the coordinating carboxylate. In this case too, no resonances below 2800 and above 3400 G were observed. Analogously to **1**, the EPR spectra of the polycrystalline complex **2** are rhombic. The resolution increases significantly from 298 to 77 K (Figure 8). The values of the *g* factor are reported in Table 5. The *R* values

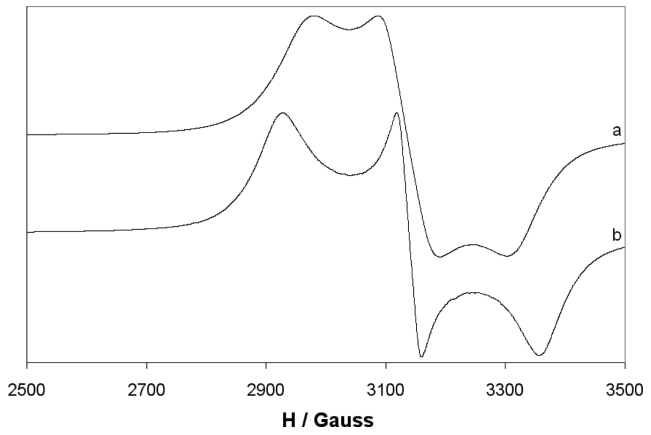

Figure 8. X-band EPR spectra of the polycrystalline complex **2** at (a) 298 and (b) 77 K.

are 1.03 and 1.11 at RT and 77 K, respectively, suggesting a slight predominance of the d_{z^2} orbital. These data are in agreement with the solid-state structure, which is characterized by a τ value of 0.51−0.53. The variation in the EPR spectra may be arising from spin transition from the $S = 1$ state to the $S = 2$ exited state. (Notably, none of the spin states in the tetranuclear complex is half-integer ($S = 1/2$). The possible spin states in **2** are $S = 0$, $S = 1$, and $S = 2$).[24]

Differently from **1**, when **2** is dissolved in an organic solvent, the same type of behavior is observed (Figure 9): in DMF, DMSO, and CH_3CN a "tetragonal" spectrum is revealed with $g_z > g_x = g_y > g_e$. The difference can be ascribed to the absence of the carboxylic group in position 4 of the aromatic ring. EPR parameters of **2** in DMF, DMSO, and CH_3CN resemble closely those of **1** in DMF and DMSO with A_z in the range of 176−178 × 10^{-4} cm^{-1} and g_z in the range of 2.264−2.277 (Table 6). These are distinctive of a $d_{x^2-y^2}$ ground state.[22]

Thermogravimetric Analysis. Thermal stabilities of the two complexes **1** and **2** were carried out by TGA. The TGA curves of **1** and **2** show a three-step degradation (Figure 10). The first degradation at the temperature range of 80−210 °C corresponds to the weight loss of 7.8% in agreement with the calculated mass loss of 7.5% for the release of methanol. But in the case of **2**, the first degradation of **1** within the temperature range of 100−140 °C corresponds to the weight loss of 5% in agreement with the calculated mass loss of 4.89% corresponding to release of water. Complex **1** undergoes a second degradation at 226 °C with sudden change in 22% mass loss up

dx.doi.org/10.1021/ic500377w | Inorg. Chem. 2014, 53, 6665−6674

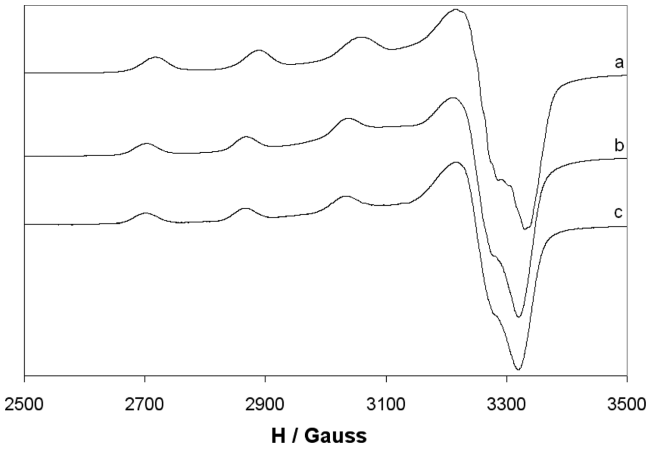

Figure 9. Anisotropic X-band EPR spectra of complex **2** dissolved in (a) DMF, (b) DMSO, and (c) CH_3CN.

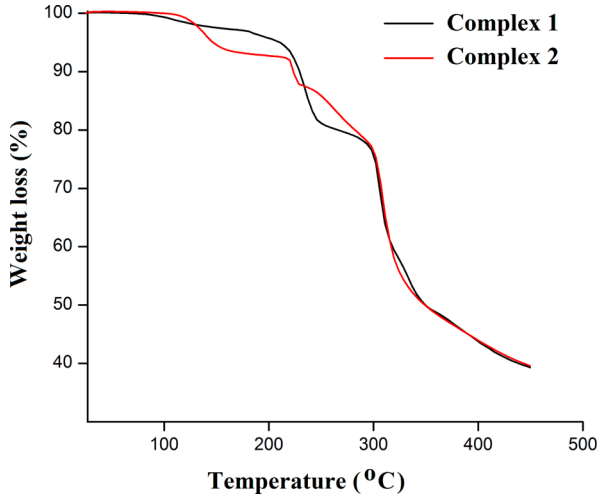

Figure 10. TGA curves for **1** and **2**.

to 290 °C with decomposition of nitrate anions, after which it undergoes a third degradation without any sudden change in mass loss up to 450 °C for **1**. Complex **2** undergoes a second and third degradation with sudden change in 22% mass loss up to 290 °C with release of nitrate anions, after which it undergoes a fourth degradation gradually without any sudden change in mass loss up to 450 °C. MSDA analysis reveals that methanol evaporates from **1** at lower temperature than water evaporates from complex **2**. Slight depression of curve for **1** is due to the evaporation of methanol at lower temperature than water from **2**, but the stable metal−organic framework of compound **1** is degraded at higher temperature than that of compound **2**.

CONCLUSION

Two copper(II) 1D cationic polymeric complexes, namely, $\{[Cu(HPymat)(MeOH)](NO_3)\}_n$ (**1**) and $\{[Cu_4(Pymab)_4(H_2O)_4]\ (NO_3)_4\}$ (**2**), were synthesized. The complex $\{[Cu(HPymat)(MeOH)](NO_3)\}_n$ (**1**) shows rhombic EPR spectra in solid state at RT and 77 K. Compound **1** shows tetragonal EPR spectra in DMSO and DMF and inverse EPR spectrum in CH_3CN. The complex $\{[Cu_4(Pymab)_4(H_2O)_4]\text{-}(NO_3)_4\}$ (**2**) shows rhombic EPR spectra in solid state at RT and 77 K and tetragonal spectra in DMSO, DMF, and CH_3CN. TGA and MSDA analyses show that complex **1** is more thermally stable than complex **2**. The Cu−N_{im} bond is more sensitive to the nature of the electronic ground state and structural distortion of the copper(II) complex. The electron-withdrawing effect of the carboxylic acid group in compound **1** weakens the Cu−O and/or Cu−N bonds and induces the flip of electronic ground state in Cu(II) ion from $d_{x^2-y^2}$ to d_{z^2}. Simple deprotonation of carboxylic acid groups causes the transformation of the distorted TBP into the distorted SQP geometry in Cu(II) complex and structural diversity.

ASSOCIATED CONTENT

Supporting Information

Differential scanning calorimetry, tables of hydrogen bonding, figures of complexes, mass spectra, powder XRD spectra, and crystallographic data in CIF format. This material is available free of charge via the Internet at http://pubs.acs.org.

AUTHOR INFORMATION

Corresponding Author

*E-mail: samiranju92@gmail.com. Tel: + 91-33-2414 6666 (Extn. 2779). Fax: + 91-33-2414 6414.

Notes

The authors declare no competing financial interest.

ACKNOWLEDGMENTS

A.S. acknowledges Council of Scientific and Industrial Research (CSIR), New Delhi, Government of India, for awarding Senior Research Fellowship (SRF) to him [CSIR Sanction No. 09/096/0586/2009-EMR-I].

REFERENCES

(1) Halcrow, M. A. *Chem. Soc. Rev.* **2013**, *42*, 1784−1784.
(2) Ovcharenko, V. I.; Romanenko, G. V.; Maryunina, K. Yu.; Bogomyakov, A. S.; Gorelik, E. V. *Inorg. Chem.* **2008**, *47*, 9537−9541.
(3) Romanenko, G. V.; Maryunina, K. Yu.; Bogomyakov, A. S.; Sagdeev, R. Z.; Ovcharenko, V. I. *Inorg. Chem.* **2011**, *50*, 6597−6609.
(4) Bousseksou, A.; Molnar, G.; Salmon, L.; Nicolazzi, W. *Chem. Soc. Rev.* **2011**, *40*, 3313−3335.
(5) Fedin, M.; Ovcharenko, V.; Sagdeev, R.; Reijerse, E.; Lubitz, W.; Bagryanskaya, E. *Angew. Chem., Int. Ed.* **2008**, *47*, 6897−6899.
(6) Okazawa, A.; Hashizume, D.; Ishida, T. *J. Am. Chem. Soc.* **2010**, *132*, 11516−11524.
(7) Halcrow, M. A. *Dalton Trans.* **2003**, 4375−4384 and references therein.
(8) Holland, J. M.; Liu, X.; Zhao, J. P.; Mabbs, F. E.; Kilner, C. A.; Thornton-Pett, M.; Halcrow, M. A. *J. Chem. Soc., Dalton Trans.* **2000**, 3316−3324.
(9) Solanki, N. K.; McInnes, E. J. L.; Mabbs, F. E.; Radojevic, S.; McPartlin, M.; Feeder, N.; Davies, J. E.; Halcrow, M. A. *Angew. Chem., Int. Ed.* **1998**, *37*, 2221−2223.
(10) Docherty, R.; Tuna, F.; Kilner, C. A.; McInnes, E. J. L.; Halcrow, M. A. *Chem. Commun.* **2012**, *48*, 4055−4057.
(11) Solanki, N. K.; Leech, M. A.; McInnes, E. J. L.; Mabbs, F. E.; Howard, J. A. K.; Kilner, C. A.; Rawson, J. M.; Halcrow, M. A. *J. Chem. Soc., Dalton Trans.* **2002**, 1295−1301.
(12) Halcrow, M. A.; Kilner, C. A.; Wolowska, J.; McInnes, E. J. L.; Bridgeman, A. J. *New J. Chem.* **2004**, *28*, 228−233.
(13) Solanki, N. K.; Leech, M. A.; McInnes, E. J. L.; Zhao, J. P.; Mabbs, F. E.; Feeder, N.; Howard, J. A. K.; Davies, J. E.; Rawson, J. M.; Halcrow, M. A. *J. Chem. Soc., Dalton Trans.* **2001**, 2083−2088.
(14) Sasmal, A.; Saha, S.; Gomez-Garcia, C. J.; Desplanches, C.; Garribba, E.; Bauza, A.; Frontera, A.; Scott, R.; Butcher, R. J.; Mitra, S. *Chem. Commun.* **2013**, *49*, 7806−7808.
(15) *WINEPR SimFonia*, Version 1.25; Bruker Analytische Messtechnik GmbH: Karlsruhe, Germany, 1996.

(16) Bruker. *SADABS, SMART, and SAINT;* Bruker AXS, Inc.: Madison, WI, 2000, 2008.
(17) Altomare, A.; Burla, M. C.; Camalli, M.; Cascarano, G. L.; Giacovazzo, C.; Guagliardi, A.; Moliterni, A. G. G.; Polidori, G.; Spagna, R. *J. Appl. Crystallogr.* **1999**, *32*, 115−119.
(18) Sheldrick, G. M. *Acta Crystallogr.* **2008**, *A64*, 112−122.
(19) (a) Farrugia, L. J. *J. Appl. Crystallogr.* **1997**, *30*, 565. (b) Keller, E. *SCHAKAL, Program for Plotting Molecular and Crystal Structures;* University of Freigburg: Freigburg, Germany, 1988.
(20) Addison, A. W.; Rao, T. N.; Reedijk, J.; van Rijn, J.; Verschoor, G. C. *J. Chem. Soc., Dalton Trans.* **1984**, 1349−1356.
(21) (a) Hathaway, B. J.; Billing, D. E. *Coord. Chem. Rev.* **1970**, *5*, 143−207. (b) Hathaway, B. J. *Struct. Bonding (Berlin)* **1984**, *57*, 55−118.
(22) Garribba, E.; Micera, G. *J. Chem. Educ.* **2006**, *83*, 1229−1232.
(23) Fereday, R. J.; Hodgson, P.; Tyagi, S.; Hathaway, B. J. *J. Chem. Soc., Dalton Trans.* **1981**, 2070−2077.
(24) Dey, S. K.; Bag, B.; Malik, K. M. A.; El Fallah, M. S.; Ribas, J.; Mitra, S. *Inorg. Chem.* **2003**, *42*, 4029−4035.

■ NOTE ADDED AFTER ASAP PUBLICATION

This paper was published on the Web on June 9, 2014, with a minor text error in the first sentence of the Abstract, along with errors in Table 5, column 7. The corrected version was reposted on June 10, 2014.